

See discussions, stats, and author profiles for this publication at: <https://www.researchgate.net/publication/254810818>

A multivalent hexapod having 24 stereogenic centers: Chirality and conformational dynamics in homochiral and heterochiral systems

ARTICLE in CRYSTENGCOMM · SEPTEMBER 2011

Impact Factor: 4.03 · DOI: 10.1039/C1CE05433C

CITATIONS

5

READS

29

6 AUTHORS, INCLUDING:



Hong Xu

Chongqing Medical University

43 PUBLICATIONS 666 CITATIONS

[SEE PROFILE](#)



Martin Wolffs

DSM

26 PUBLICATIONS 1,342 CITATIONS

[SEE PROFILE](#)



Albertus P H J Schenning

Technische Universiteit Eindhoven

295 PUBLICATIONS 14,360 CITATIONS

[SEE PROFILE](#)



Steven De Feyter

University of Leuven

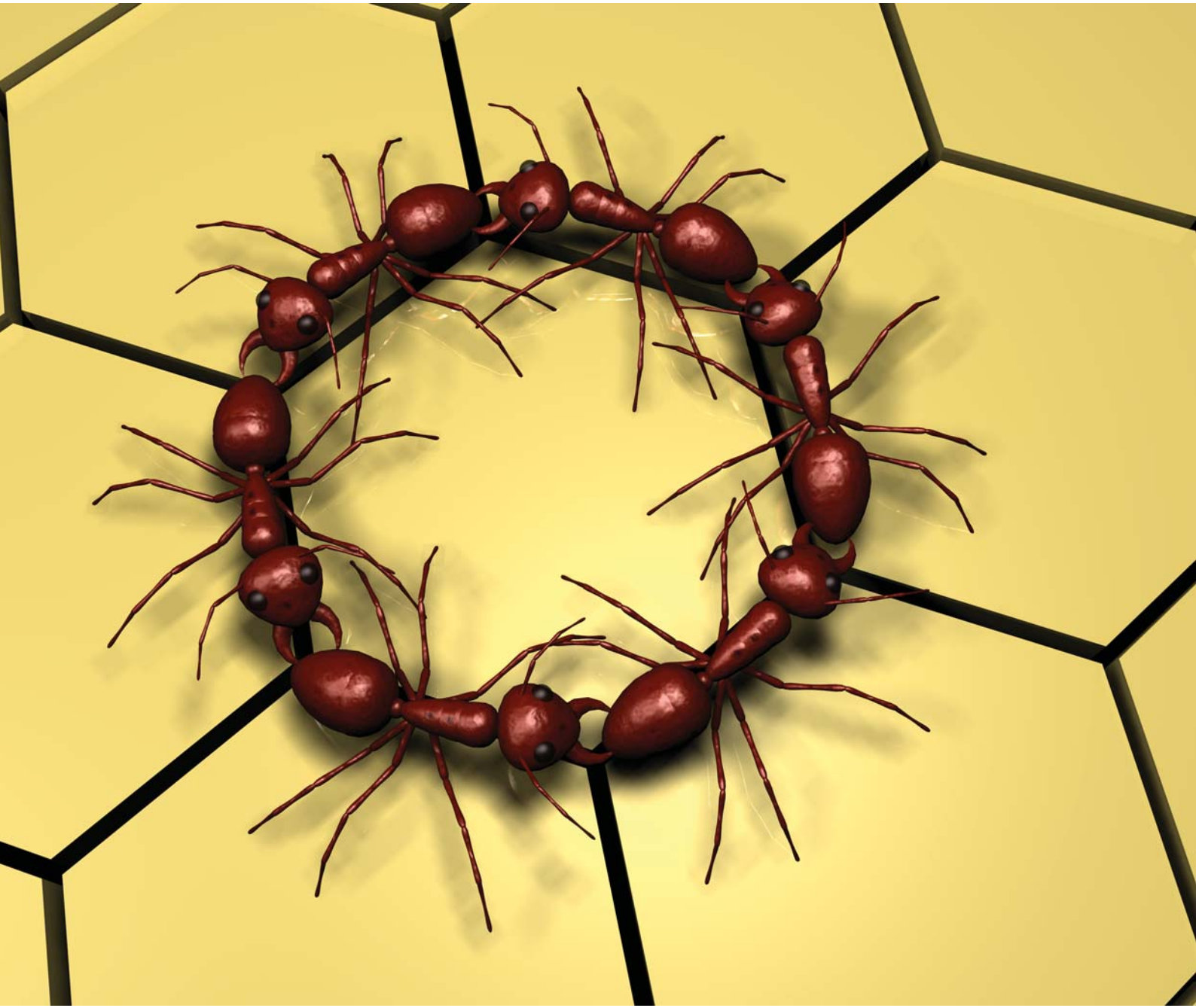
326 PUBLICATIONS 9,691 CITATIONS

[SEE PROFILE](#)

CrystEngComm

www.rsc.org/crystengcomm

Volume 13 | Number 18 | 21 September 2011 | Pages 5521–5598



COVER ARTICLE

Wuest *et al.*

Engineering homologous molecular organization in 2D and 3D.
Cocrystallization of aminoazines and alkanecarboxylic acids

RSC Publishing

This paper is published as part of a *CrystEngComm* themed issue entitled:

2D Crystal Engineering

Guest Editors: Neil Champness and Steven De Feyter

Published in issue 18, 2011 of *CrystEngComm*



Image reproduced with permission of Steven de Feyter

Other articles published in this issue include:

[Nanopatterning the graphite surface with ordered macrocyclic or ribbon-like assemblies of isocytosine derivatives: an STM study](#)

Artur Ciesielski, Silvia Colella, Leszek Zalewski, Bernd Bruchmann and Paolo Samorì
CrystEngComm, 2011, DOI: 10.1039/C1CE05521F

[Engineering homologous molecular organization in 2D and 3D. Cocrystallization of aminoazines and alkanecarboxylic acids](#)

Adam Duong, Thierry Maris and James D. Wuest
CrystEngComm, 2011, DOI: 10.1039/C1CE05445G

[Chiral non-periodic surface-confined molecular nanopatterns revealed by scanning tunnelling microscopy](#)

Wojciech J. Saletra, Hong Xu, Tom Vosch, Steven De Feyter and David B. Amabilino
CrystEngComm, 2011, DOI: 10.1039/C1CE05403A

Visit the *CrystEngComm* website for more cutting-edge crystal engineering research

www.rsc.org/crystengcomm

Cite this: *CrystEngComm*, 2011, **13**, 5584

www.rsc.org/crystengcomm

PAPER

A multivalent hexapod having 24 stereogenic centers: chirality and conformational dynamics in homochiral and heterochiral systems

Hong Xu,^a Martin Wolffs,^b Željko Tomović,^b E. W. Meijer,^b Albertus P. H. J. Schenning^{*b} and Steven De Feyter^{*a}

Received 11th April 2011, Accepted 9th June 2011

DOI: 10.1039/c1ce05433c

The monolayer formation of a chiral oligo(*p*-phenylene vinylene)-substituted hexaarylbenzene with 24 stereogenic centers is investigated at the interface between a liquid and a solid substrate, highly oriented pyrolytic graphite. Scanning tunneling microscopy (STM) reveals that molecular chirality is expressed at the supramolecular level. When both enantiomers are co-adsorbed on the surface, a racemic conglomerate is formed. Both enantiomers and their mixtures show interesting conformational and translational dynamics at the liquid-solid interface, giving insight into expression of chirality, nucleation and monolayer growth.

Introduction

Two-dimensional molecular engineering deals with the understanding of and the control over molecular adsorption on surfaces.^{1–5} As it turns out, molecular ordering can not only be controlled by non-covalent molecule-molecule interactions or molecule-substrate interactions (typically van der Waals),^{6–8} but also structural aspects such as chiral centers play a decisive role on the outcome of the two-dimensional (2D) self-assembly process.^{9–12}

When Pasteur realised in 1848 that two enantiomers, *i.e.* mirror-image type molecules, do not always co-crystallise in racemates but might crystallise in different, though mirror-image related conglomerate crystals, an important step was taken in the mechanical (manual) separation of mirror-image molecules.¹³ The separation of such mirror-image molecules, also called optical antipodes,¹⁴ is a major issue in the pharmaceutical industry, especially if the synthesis of enantiomerically pure compounds turns out to be impossible. Most of those separation processes involve the interaction of the target molecules with a chiral surface, which is very often made chiral by the (covalent) adsorption of chiral molecules.^{15,16}

Thanks to scanning tunneling microscopy (STM), much information has been obtained on the influence of molecular chirality on the self-assembly of molecules into monolayers onto atomically-flat conductive surfaces, both under ultrahigh vacuum conditions as well as under ambient conditions or at the

liquid-solid interface.^{17–20} In addition, STM can provide information on the molecular dynamics involved.^{21,22}

While most studies deal with the self-assembly of molecules with one chiral center, we have recently reported on the self-assembly of an enantiopure molecule which contains 24 identical chiral centers.²³ This *S*-enantiomer (**S-1**, Fig. 1) was shown to express its chirality in the self-assembly process. In addition, some unique conformational and translational dynamics could be documented.²⁴

In this paper, we report on the self-assembly, chiral expression and dynamics of both enantiomers (Fig. 1) and their mixtures at the liquid-solid interface, with a focus on the events taking place at domain boundaries.^{25–28}

Experimental section

Materials

The *S*-enantiomer, **S-1**, was synthesized according to our earlier reported procedure²⁴ while the synthesis of the *R*-enantiomer, **R-1**, will be published elsewhere.

Scanning tunneling microscopy

PicoSPM (Agilent) (using the constant-current mode) was used for performing STM experiments. Mechanical cut tips were used in the measurements. The compounds under investigation were dissolved in 1-phenyloctane (Aldrich) at a concentration of approximately 10^{–4} M and a drop of this solution (*ca.* 0.05 ml) was applied on a freshly cleaved surface of highly oriented pyrolytic graphite (HOPG) (grade ZTB, Advanced Ceramics Inc., Cleveland, OH). Then, the STM tip was immersed into the solution and the surface was scanned: a bright (dark) contrast refers to a high (low) height. The bias voltage was applied to the

^aDepartment of Chemistry, Laboratory of Molecular and Nanomaterials, Katholieke Universiteit Leuven, Celestijnenlaan 200F, 3001 Leuven, Belgium. E-mail: Steven.DeFeyter@chem.kuleuven.be

^bLaboratory of Macromolecular and Organic Chemistry, Eindhoven University of Technology, P. O. Box 513, 5600MB Eindhoven, the Netherlands. E-mail: A.P.H.J.Schenning@tue.nl

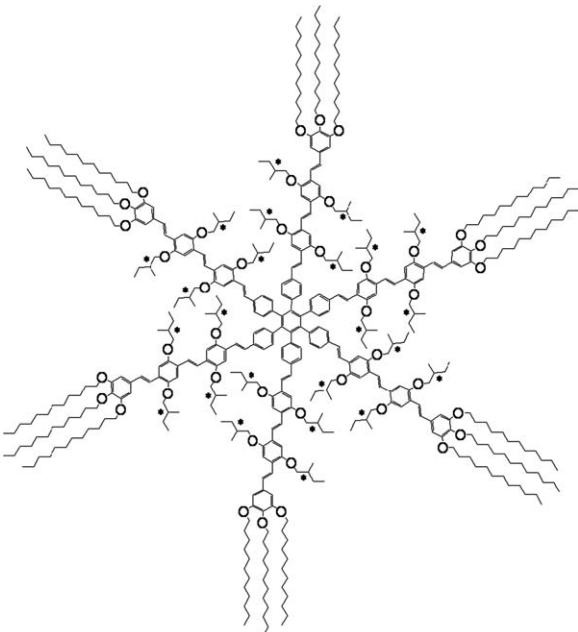


Fig. 1 Chemical structure of the oligo(*p*-phenylene vinylene)-substituted hexaarylbenzene **1** having 24 stereogenic centers. **S-1** has 24 *S*-2-methylbutoxy side chains while **R-1** has 24 *R*-2-methylbutoxy side chains.

sample in such a way that, at negative bias voltage, electrons tunnel from the sample to the tip.

Results and discussion

Upon applying a drop of a solution on top of the graphite substrate, after about 30 min the spontaneous formation of a monolayer sets in. STM images of monolayers of both enantiomers of **1** at the 1-phenyloctane–HOPG interface are shown in Fig. 2. The main structural characteristics of the molecules can easily be appreciated. The oligo(*p*-phenylene vinylene) (OPV) units appear as bright rods in the STM images. Dodecyl chains can be recognized as faint bright lines running perpendicular to the OPV units. Only two out of three alkyl chains can be identified, suggesting that the third one is directed towards the supernatant solution. Details of the organization of **S-1** have been reported before.²³ The organization of the newly investigated **R-1** is identical to that of **S-1**, except for symmetry and chirality aspects. Unit cell parameters are summarized in Table 1. The STM images are two-dimensionally (2D) chiral, and the molecules appear as stars, which belong to the plane group 6mm (the combination of a mirror with a hexad axis). Neglecting the intrinsic chirality of the molecules, these stars can only order into an achiral pattern if their “arms” are oriented parallel or perpendicular to the unit cell vectors. This is, however, not the case, and this has an effect on the relative distance between parallel oriented OPV-units of adjacent molecules. Consider, for instance, the orientation of the long black and short white lines that connect the terminal phenyl groups of similarly oriented OPV units along unit cell vector *b* in Fig. 2A & B. Note that these marker lines are not in line, and that the relative orientation of the black and white rods is opposite for both enantiomers. **1** self-assembles into a chiral pattern in accordance with the plane group *p*6. As expected, **S-1** and **R-1** form mirror image patterns.

This enantiomorphism is not only expressed at the level of the molecular organization within the monolayer. A more subtle expression of the different chirality is the monolayer registry with respect to the graphite substrate. The graphite lattice templates the monolayer formation. The unit cell vectors are rotated by about $\theta = +2 \pm 2^\circ$ (for **S-1**) or $\theta = -3 \pm 3^\circ$ (for **R-1**) with respect to the main symmetry axes of HOPG, *i.e.* the equivalent $<1\ 2\ 1\ 0>$ directions. Note though that there are also domains where the alkyl chains are not aligned along the main symmetry axes of graphite, and where the angle θ is larger. However, these observations were typically made within 30 min after dropcasting, and in time, regular domains as the ones described above prevail.

Tentative models (Fig. 3) show that alkyl chains at the end of each leg interact with the ones coming from adjacent molecules and act as “locks” to stabilize the monolayer. The orientation of the alkyl chains with respect to the OPV cores is the opposite for both enantiomers. For **S-1**, alkyl chains are rotated ‘clockwise’ (CW) with respect to the OPV core while alkyl chains in **R-1** are rotated ‘counterclockwise’ (CCW).

Depositing a mixture of both enantiomers of **1** leads apparently to a conglomerate: the domains reflect those of the pure enantiomers in terms of appearance and unit cell parameters. Therefore, we conclude that domains are exclusively composed of **S-1** or **R-1** (Fig. 2D). Indeed, after mixing both enantiomers at a ratio of **S-1** (7):**R-1** (3) and dropcasting the solution onto HOPG, clear “*S*-type” and “*R*-type” domains can be distinguished. About half of the molecules self-assemble into disordered areas which is more than for the enantiopure systems. Disordered domains (*e.g.* Fig. 2C) are defined as domains where the centers of the molecules do not coincide with lattice points, *i.e.* they are not part of a regular 2D lattice.

Previously, we have reported extensively on the conformational and translational dynamics of physisorbed **S-1** molecules in 2D crystalline domains and in disordered areas.²⁴ The appearance of some molecules changes in time, *i.e.* they undergo conformational changes, and in disordered areas, often translational dynamics was observed.

R-1 shows very similar conformational and translational dynamics. About 74% of **R-1** molecules are self-assembled in ordered domains. The desorption/readsoption or reorientation of one or two OPV-legs leads to the observation of defect-like molecules. Here we define a molecule as being a ‘defect’ one as either part of the molecule is not visible or perfectly oriented, because of conformational dynamics. As shown in Fig. 4, molecules can be clearly distinguished as molecules with 6 OPV-legs (6-leg) or less (5-leg, 4-leg, or unidentified). As shown before, this was attributed to OPV-legs which are not adsorbed on the surface but are solvated. In time, the same molecule can adopt several conformational states, as was reported extensively for **S-1**.²⁴

In monolayers formed by dropcasting from a mixture of **S-1** and **R-1**, both well ordered *S*- and *R*-domains can be observed and within these 2D crystals, 97.5% of molecules appear as hexapods. The results of the data analysis are summarized in Table 2.

At first glance, the data analysis for **S-1**, **R-1** and a 7:3 mixture of **S-1** and **R-1** shows quite similar results, except for the percentage of molecules appearing in ordered *versus*

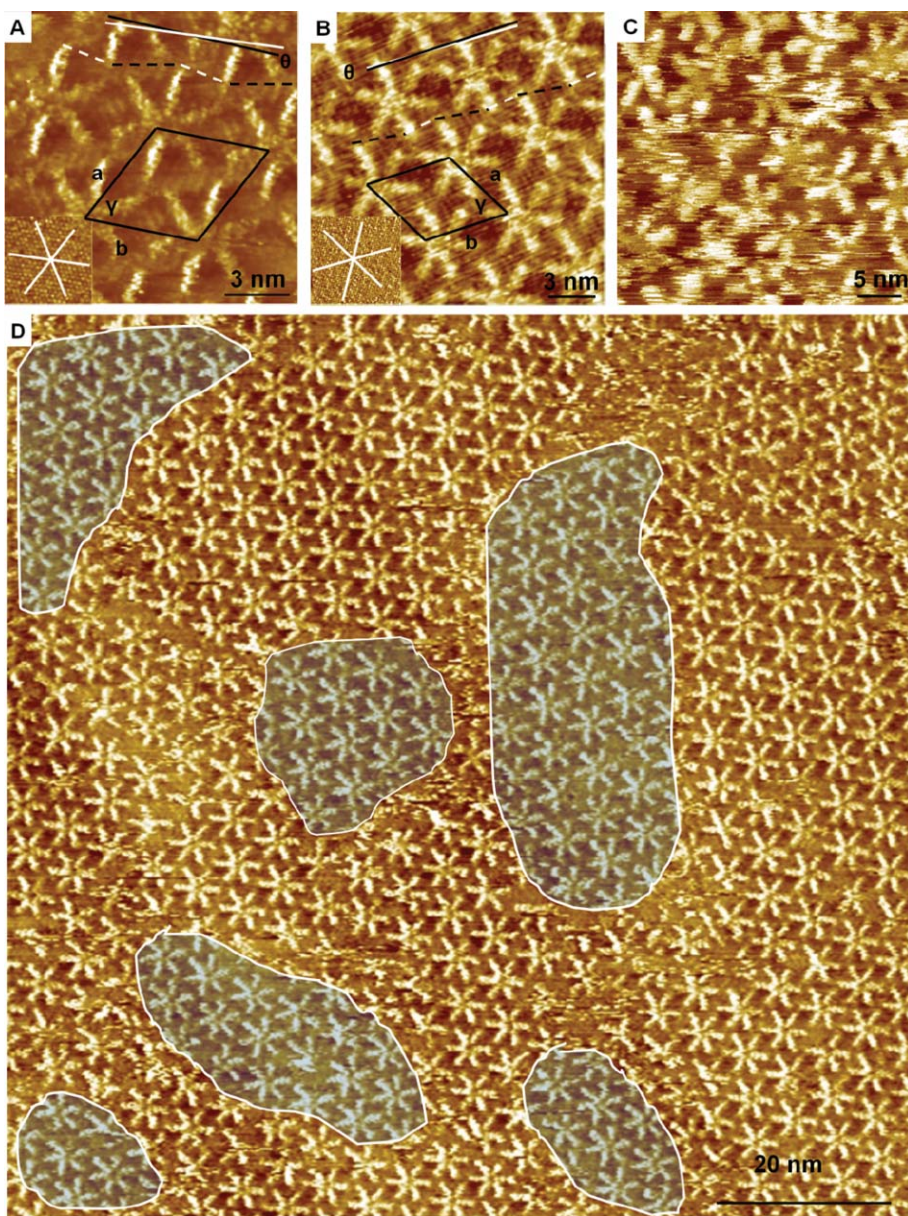


Fig. 2 STM images of **1** physisorbed at the 1-phenyloctane–HOPG interface. (A) **S-1** ($I_{set} = 0.05 \text{ nA}$; $V_{set} = -0.8 \text{ V}$); (B) **R-1** ($I_{set} = 0.2 \text{ nA}$; $V_{set} = -0.8 \text{ V}$); (C) a disordered domain formed by **S-1** ($I_{set} = 0.05 \text{ nA}$; $V_{set} = -0.8 \text{ V}$); (D) a 7 : 3 mixture of **S-1** and **R-1** ($I_{set} = 0.2 \text{ nA}$; $V_{set} = -0.8 \text{ V}$). The insets show STM images of HOPG (not to scale) corresponding with sites underneath the monolayer ($I_{set} = 0.2 \text{ nA}$; $V_{set} = -0.001 \text{ V}$). The unit cell is indicated in black. The solid white lines coincide with the direction of the main symmetry axes of HOPG, *i.e.* $\langle 1 -2 1 0 \rangle$. The short white and long dashed black lines connect the terminal phenyl groups of similarly oriented OPV units along unit cell vector b . **R-1** domains are marked in (D).

Table 1 Structural parameters of the monolayer packing. Unit cell parameters (a , b , γ), and θ , the angle of a unit cell vector with respect to a main symmetry axis of HOPG

| | a/nm | b/nm | $\gamma/^\circ$ | $\theta/^\circ$ |
|------------|---------------|---------------|-----------------|-----------------|
| S-1 | 5.7 ± 0.1 | 5.7 ± 0.1 | 59 ± 1 | $+2 \pm 2$ |
| R-1 | 5.7 ± 0.2 | 5.7 ± 0.1 | 59 ± 3 | -3 ± 3 |

disordered domains, which is much lower for the mixture compared to the enantiopure systems. Otherwise, the same trends are observed. The distribution of the so-called defect molecules, actually conformational isomers, in ordered and

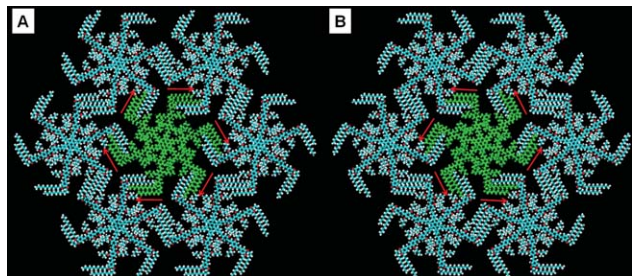


Fig. 3 Tentative models of homochiral domains formed by **1**. (A) **S-1**; (B) **R-1**. Red arrows indicate the ‘orientation’ of the alkyl chains.

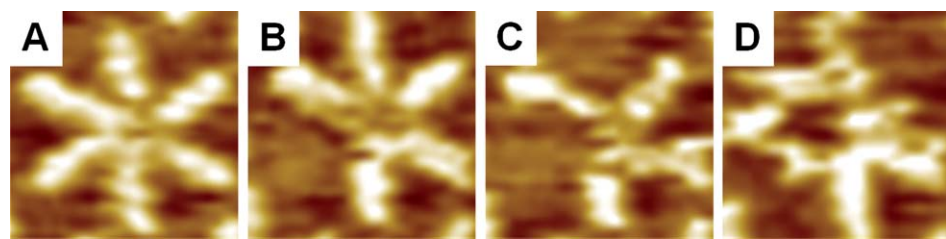


Fig. 4 Zoomed STM images of *R*-**1** molecules with different appearance. (A) 6-leg; (B) 5-leg; (C) 4-leg; (D) undefined. These differences in appearances reflect conformational differences, where one or more OPV-legs are temporarily desorbed.

disordered domains is quite different. In ordered patterns, over 90% of the hexapods appear as perfectly aligned molecules, while in disordered areas, 5-leg species dominate the monolayer composition. Furthermore, in ordered domains, the possibility to observe a dimer defect (40% for *S*-**1** and *R*-**1**, 33% for a mixture of *S*-**1** and *R*-**1**), *i.e.* two defect-like molecules adjacent to each other, is higher than theoretically expected (27%), indicating that a defect molecule promotes the presence of another one in its periphery.

In the following, we will focus on what happens at domain boundaries. As the mixture of *S*-**1** and *R*-**1** forms a conglomerate, any differences between the mixture and the enantiopure systems are expected to show up at domain boundaries. Independent of the solution composition (*R*-**1**, or *S*-**1** or a mixture of *R*-**1** and *S*-**1**), there are two cases which can be observed at domain boundaries between two *ordered domains* (Fig. 5). While similar phenomena can be observed at boundaries between homochiral domains, we illustrate these two cases for domain boundaries of heterochiral domains:

1) Molecules in adjacent domains self-assemble without orientational changes at domain boundaries. The domain boundary is ordered. If the distance between centers of two adjacent molecules which belong to two different domains is larger than a unit cell vector, a cavity can be observed without any molecules adsorbed (Fig. 5B). Another case is when two

adjacent molecules from different domains get even closer than a unit cell vector, while they still appear as perfectly aligned molecules (Fig. 5C).

2) Molecules at a domain boundary are disordered showing defects (Fig. 5D).

Fig. 5 is a representative image of part of a monolayer formed from a solution mixture of *S*-**1** and *R*-**1**. The identity of each molecule, *i.e.* absolute configuration and conformational status, is presented by colored symbols.

The averaged domain size obviously affects the chance to observe domain boundaries. The smaller the domains, the more domain boundaries. This is reflected by the parameter M:B: the ratio of the number of molecules adsorbed in ordered domains (M) and in domain boundaries (B). Domains in enantiopure systems are larger and very few domain boundaries can be observed. In heterochiral systems, M:B for domain boundaries involving homochiral domains (*S-S* and *R-R*) is smaller than in enantiopure systems which indicates the smaller size of the domains. At heterochiral domain boundaries, it is not possible for molecules to self-assemble in the same way as in ordered domains. Table 3 reflects the number of molecules in the bulk of domains and at domain boundaries, for the enantiopure as well as for the enantiomixed monolayers, differentiating in the nature of the domain boundary (homochiral (*S-S* and *R-R*) or heterochiral (*R-S*)).

Table 2 Summary of the data analysis of monolayers formed by *S*-**1**, *R*-**1** or a 7 : 3 mixture of *S*-**1** and *R*-**1**. Ordered domains refer to sites where the molecules are apparently part of a 2D crystalline lattice, neglecting conformational differences. In disordered domains, the center of mass of the molecules does not coincide with a 2D crystal lattice point. For each case, the number of observations is indicated, together with the % in parentheses. ‘Isolated’ refers to the situation where a so-called ‘defect’-molecule, *i.e.* a conformational isomer with less than 6 OPV-legs adsorbed on the HOPG surface, is not surrounded by other ‘defect’ molecules. In contrast, ‘dimer’ refers to ‘defect’-molecules which are surrounded by another ‘defect’-molecule, but not necessarily of the same type

| | | <i>S</i> - 1 | <i>R</i> - 1 | <i>S</i> - 1 + <i>R</i> - 1 |
|------------------------------------|--------------------|---------------------|---------------------|---|
| Ordered domains | 6-leg | 13398 (95.5%) | 6739 (93.9%) | 6982 (97.5%) |
| | 5-leg isolated | 289 (2.1%) | 206 (2.9%) | 94 (1.3%) |
| | 4-leg isolated | 51 (0.4%) | 38 (0.5%) | 20 (0.3%) |
| | Undefined isolated | 39 (0.3%) | 19 (0.3%) | 6 (0.1%) |
| | 5-leg dimer | 179 (1.3%) | 137 (1.9%) | 45 (0.6%) |
| | 4-leg dimer | 46 (0.3%) | 28 (0.4%) | 7 (0.1%) |
| | Undefined dimer | 31 (0.2%) | 11 (0.2%) | 6 (0.1%) |
| Disordered domains | 6-leg | 890 (14.1%) | 360 (14.6%) | 385 (6.4%) |
| | 5-leg | 2176 (34.5%) | 1081 (43.9%) | 2559 (42.6%) |
| | 4-leg | 737 (11.7%) | 317 (12.9%) | 915 (15.2%) |
| | Undefined | 2512 (39.8%) | 706 (28.7%) | 2150 (35.8%) |
| Total images | | 60 | 22 | 30 |
| Total molecules | | 20348 | 9642 | 13169 |
| Order : disorder | | 2.2 : 1 | 2.9 : 1 | 1.2 : 1 |
| 5-leg : 4-leg in ordered domain | | 4.8 : 1 | 5.2 : 1 | 5.1 : 1 |
| Isolated : dimer in ordered domain | | 1.5 : 1 | 1.5 : 1 | 2.1 : 1 |

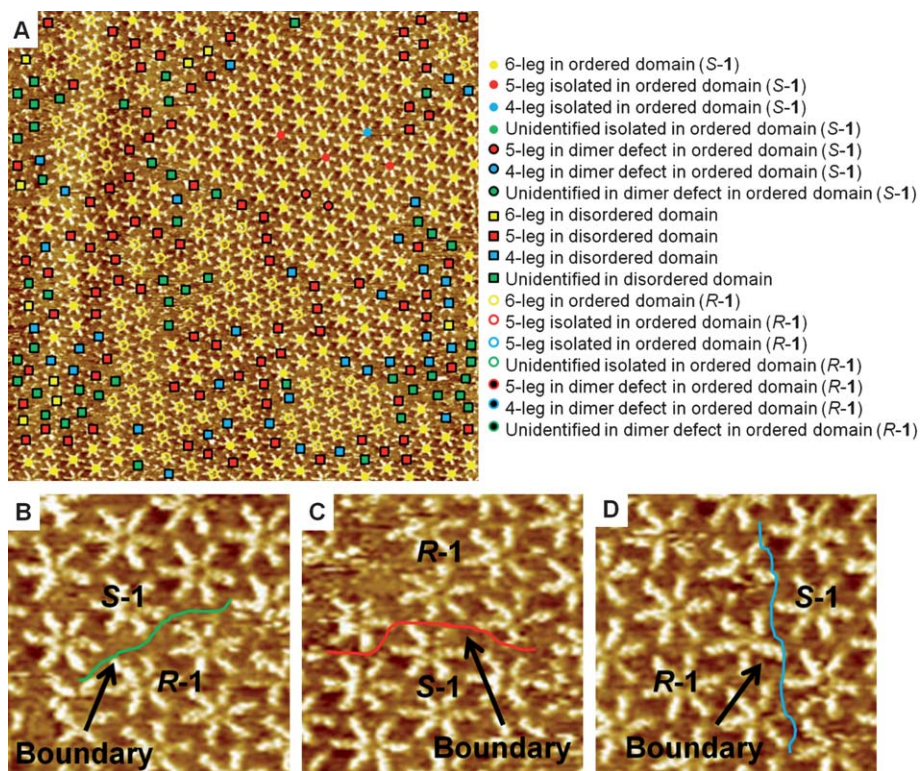


Fig. 5 STM images of a monolayer formed by physisorption from a 3 : 7 mixture of *R*-1 and *S*-1 physisorbed at the 1-phenyloctane–HOPG interface. (A) Color-coded large-scale STM image ($103.8 \times 103.8 \text{ nm}^2$). The center of a molecule is indicated by a disk (ordered *S*-domain), a circle (ordered *R*-domain) or square (disordered area). Disks with black edge indicate dimer defects in ordered *S*-domains while disks without black edges indicate isolated defects in ordered *S*-domains. Circles with black center indicate dimer defects in ordered *R*-domains while circles without black center indicate isolated defects. The color refers to the number of visible OPV legs: yellow (6); red (5); blue (4); green (undefined). Domain boundaries are marked as regions with different color in B, C, and D.

Table 3 Population of molecules in the bulk of ordered domains and at domain boundaries for the enantiopure systems, and the 7 : 3 mixture of both enantiomers

| | Mixture of <i>S</i> -1 and <i>R</i> -1 | | | <i>S</i> -1 | <i>R</i> -1 |
|--|--|---------------------|---------------------|---------------------|---------------------|
| | <i>S</i> - <i>R</i> | <i>S</i> - <i>S</i> | <i>R</i> - <i>R</i> | <i>S</i> - <i>S</i> | <i>R</i> - <i>R</i> |
| Number of molecules at domain boundaries (B) | 1375 | 134 | 76 | 246 | 103 |
| Number of molecules in ordered domains (M) | 7160 | 5062 | 2098 | 14033 | 7178 |
| M:B | 5.2 : 1 | 37.8 : 1 | 27.6 : 1 | 57.0 : 1 | 69.7 : 1 |

Some molecules which adsorb on the surface first act as the “seeds” of an ordered domain and more molecules self-assemble around these “seeds”. Due to the molecule-molecule and molecule-surface interactions, in combination with Ostwald ripening,^{29,30} domains stabilize and expand. Molecules at the periphery of a domain will finally meet the ones from a growing adjacent domain.

For monolayers formed from a mixture of both enantiomers, heterochiral domains cannot merge by any dynamic behavior. The position of the domain boundary may change, but the boundary won’t disappear in time just by in-plane dynamics of the molecules. From Fig. 6, we can conclude that although the enantiomeric ratio on the surface changes from site to site and

varies in time (the STM images are not recorded on the same location), the enantiomeric ratio (*S*-1:*R*-1) fluctuates around 2.3, the value of the enantiomeric ratio in solution. It indicates that both enantiomers have the same probability to self-assemble on the surface even in the case of a non-racemic mixture. The

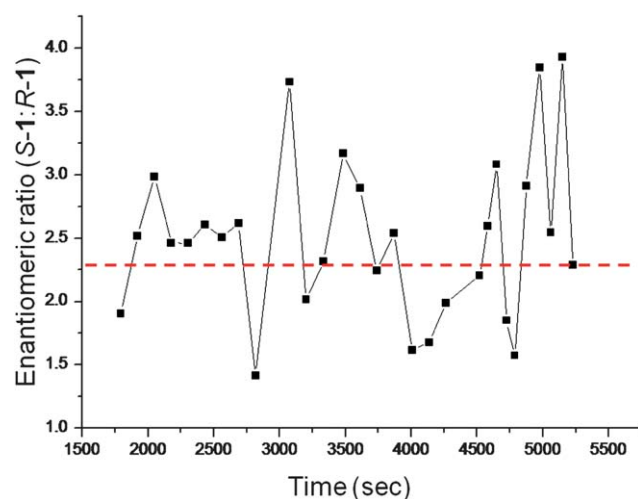


Fig. 6 Enantiomeric ratio of *S*-1:*R*-1 self-assembled at the liquid-solid interface, from a 7 : 3 heterochiral mixture in solution. The red dashed line reflects the solution composition.

Table 4 Relative importance of conformational isomers at homochiral and heterochiral domain boundaries. The label ‘defects’ refers to conformational isomers with less than six OPV legs adsorbed on the surface, as well as to conformational isomers (also 6-leg) which do not fit on top of 2D lattice points

| | | Mixture of S-1 + R-1 | | | S-1 | R-1 |
|--|--------------|----------------------|-------------|------------|-------------|------------|
| | | S-R | S-S | R-R | S-S | R-R |
| Defects | 6-leg | 13 (0.95%) | 5 (3.7%) | 1 (1.3%) | 26 (10.6%) | 16 (15.5%) |
| | 5-leg | 633 (46.0%) | 50 (37.3%) | 36 (46.4%) | 78 (31.7%) | 49 (47.6%) |
| | 4-leg | 220 (16.0%) | 21 (15.7%) | 11 (14.5%) | 22 (8.9%) | 8 (7.8%) |
| | unidentified | 192 (14.0%) | 51 (38.1%) | 27 (35.5%) | 102 (41.5%) | 26 (25.2%) |
| Perfect | bulk | 189 (13.7%) | 5 (3.7%) | 1 (1.3%) | 16 (6.5%) | 2 (1.9%) |
| | attached | 128 (9.3%) | 2 (1.5%) | 0 (0.0%) | 2 (0.8%) | 2 (1.9%) |
| Total number (%) of defect-molecules at domain boundaries | | 1058 (77.0%) | 127 (94.8%) | 75 (98.7%) | 228 (92.7%) | 99 (96.1%) |
| Total number (%) of defect-free molecules at domain boundaries | | 317 (23.0%) | 7 (5.2%) | 1 (1.3%) | 18 (7.3%) | 4 (3.9%) |

majority component can't force the minority one to adopt an unfavored packing or replace it, *i.e.* competitive adsorption, *via* a desorption-readsorption process. So, large homochiral domains are not easily formed and domain boundaries are frequently being observed.

At boundaries of domains containing molecules of the same absolute configuration, about 90% of the molecules show up as defects. The position of the boundary may change due to the conformational and translational dynamic behavior of the molecules and finally adjacent domains can merge and form a bigger domain. This explains why M:B is larger for enantiopure systems. Note that for domain boundaries of the enantiomixed system, a significantly smaller fraction of molecules appear as ‘defects’ (Table 4). This might appear counterintuitive. A possible explanation refers to the kinetics of domain growth. In case of adjacent homochiral domains, the interfacial energy is relatively low (unit cell vectors of both domains run parallel), and it is expected that the merging of two domains will occur fast, especially in case of well-aligned defect free molecules. However, we expect that domain boundaries with more defects are slower to merge. In case of heterochiral domain boundaries, there is no way that both domains can merge, reflecting the difference in population of the respective defects. Table 4 gives a detailed overview of the conformational isomers and their abundance at homochiral and heterochiral domain boundaries, for the enantiopure and enantiomixed systems.

Conclusion

In summary, molecular hexapods form distinct well-ordered chiral monolayers at the liquid-solid interface, and mixtures of both enantiomers lead to conglomerate formation, *i.e.* both enantiomers appear in separate domains. These molecules show very interesting dynamic behavior. In time, they can adopt several conformations, which is reflected by the disappearance and reappearance of one or more OPV-legs. Homochiral and heterochiral systems have been evaluated in detail, in terms of the size of the domains, the population of the different conformational states and especially, the situation at domain boundaries. It turns out that at domain boundaries between domains of the same chirality, more molecules appear as ‘defects’ compared to

domain boundaries between domains of opposite chirality, reflecting the different degree of dynamics and providing insight into the mechanism of monolayer growth. The relatively slow dynamics of this system opens opportunities to investigate the nature of the liquid-solid interface in more detail. For instance, the effect of solvents on the dynamics and temperature could be explored.

Acknowledgements

The research leading to these results has received funding from the European Community's Seventh Framework Program under grant agreement n° NMP4-SL-2008-214340, project RESOLVE. Furthermore, this work is supported by the Fund of Scientific Research – Flanders (FWO), K.U.Leuven (GOA), the Belgian Federal Science Policy Office through IAP-6/27, and the Institute for the Promotion of Innovation by Science and Technology in Flanders (IWT).

References

- 1 J. A. A. W. Elemans, S. B. Lei and S. De Feyter, *Angew. Chem., Int. Ed.*, 2009, **48**, 7298.
- 2 J. V. Barth, G. Costantini and K. Kern, *Nature*, 2005, **437**, 671.
- 3 R. Otero, F. Rosei and F. Besenbacher, *Annu. Rev. Phys. Chem.*, 2006, **57**, 497.
- 4 A. Ciesielski, C.-A. Palma, M. Bonini and P. Samorí, *Adv. Mater.*, 2010, **22**, 3506.
- 5 S. B. Lei and S. De Feyter, *Top. Curr. Chem.*, 2008, **285**, 269.
- 6 Y. L. Yang and C. Wang, *Chem. Soc. Rev.*, 2009, **38**, 2576.
- 7 A. Langner, S. L. Tait, N. Lin, C. Rajadurai, M. Ruben and K. Kern, *Proc. Natl. Acad. Sci. U. S. A.*, 2007, **104**, 17927.
- 8 C. Rohr, M. B. Gambra, K. Gruber, E. C. Constable, E. Frey, T. Franosch and B. A. Hermann, *Nano Lett.*, 2010, **10**, 833.
- 9 R. Raval, *Chem. Soc. Rev.*, 2009, **38**, 707.
- 10 J. A. A. W. Elemans, I. De Cat, H. Xu and S. De Feyter, *Chem. Soc. Rev.*, 2009, **38**, 722.
- 11 K. H. Ernst, *Curr. Opin. Colloid Interface Sci.*, 2008, **13**, 54.
- 12 N. Katsonis, E. Lacaze and B. L. Feringa, *J. Mater. Chem.*, 2008, **18**, 2065.
- 13 L. Pasteur, *Alembic Club Rep.*, 1905, **14**, 1.
- 14 E. L. Eliel, S. H. Wilen, *The Stereochemistry of Organic Compounds*, Wiley-VCH, 1994, p. 1203.
- 15 D. H. Dressler and Y. Mastai, *Chirality*, 2007, **19**, 358.
- 16 D. H. Dressler and Y. Mastai, *J. Colloid Interface Sci.*, 2007, **310**, 653.
- 17 M. Ortega Lorenzo, S. Haq, T. Bertrams, P. Murray, R. Raval and C. J. Baddeley, *J. Phys. Chem. B*, 1999, **103**, 10661.

-
- 18 M. Ortega Lorenzo, C. J. Baddeley, C. Muryn and R. Raval, *Nature*, 2000, **404**, 376.
- 19 S. De Feyter, A. Gesquière, C. Meiners, M. Sieffert, K. Müllen and F. C. De Schryver, *Langmuir*, 1999, **15**, 2817.
- 20 X. Zhang, Q. Chen, G.-J. Deng, Q.-H. Fan and L.-J. Wan, *J. Phys. Chem. C*, 2009, **113**, 16193.
- 21 F. Rosei, M. Schunack, Y. Naitoh, P. Jiang, A. Gourdon, E. Laegsgaard, I. Stensgaard, C. Joachim and F. Besenbacher, *Prog. Surf. Sci.*, 2003, **71**, 95.
- 22 M. Lingenfelder, G. Tomba, G. Costantini, L. C. Ciacchi, A. De Vita and K. Kern, *Angew. Chem., Int. Ed.*, 2007, **46**, 4492.
- 23 Ž. Tomović, J. van Dongen, S. George, H. Xu, W. Pisula, P. Leclère, M. M. J. Smulders, S. De Feyter, E. W. Meijer and A. P. H. J. Schenning, *J. Am. Chem. Soc.*, 2007, **129**, 16190.
- 24 H. Xu, A. Minoia, Ž. Tomović, R. Lazzaroni, E. W. Meijer, A. P. H. J. Schenning and S. De Feyter, *ACS Nano*, 2009, **3**, 1016.
- 25 Q. Chen, T. Chen, X. Zhang, L.-J. Wan, H.-B. Liu, Y.-L. Li and P. Stang, *Chem. Commun.*, 2009, 3765.
- 26 Q. Chen, T. Chen, D. Wang, H.-B. Liu, Y.-L. Li and L.-J. Wan, *Proc. Natl. Acad. Sci. U. S. A.*, 2010, **107**, 2769.
- 27 T. Huang, Z. Hu, B. Wang, L. Chen, A. Zhao, H. Wang and J. G. Hou, *J. Phys. Chem. B*, 2007, **111**, 6973.
- 28 M. Lackinger, S. Griessl, L. Kampschulte, F. Jamitzky and W. M. Heckl, *Small*, 2005, **1**, 532.
- 29 A. T. Hubbard, *Encyclopedia of Surface and Colloid Science*, CRC, 2004, p. 4230.
- 30 L. Ratke, P. W. Voorhees, *Growth and coarsening: Ostwald ripening in material processing*, Springer, 2002, p. 117.